Data in Brief 21 (2018) 1019–1025

Contents lists available at ScienceDirect

Data in Brief

journal homepage: www.elsevier.com/locate/dib

Data Article

Data on SD-OCT image acquisition, ultrastructural features, and horizontal tissue shrinkage in the porcine retina

Wankun Xie [a,b], Min Zhao [a,b], Shu-Huai Tsai [a], William L. Burkes [a], Luke B. Potts [b], Wenjuan Xu [a], H. Ross Payne [c], Travis W. Hein [a,b], Lih Kuo [a,b], Robert H. Rosa Jr. [a,b,*]

[a] Department of Medical Physiology, Texas A&M University Health Science Center, Temple, TX, USA
[b] Department of Ophthalmology and Ophthalmic Vascular Research Program, Scott & White Eye Institute, Temple, TX, USA
[c] Image Analysis Laboratory, Texas A&M University College of Veterinary Medicine, College Station, TX, USA

ARTICLE INFO

Article history:
Received 24 August 2018
Received in revised form
21 October 2018
Accepted 23 October 2018
Available online 27 October 2018

ABSTRACT

The data presented in this article are related to the research paper entitled "Correlation of Spectral Domain Optical Coherence Tomography with Histology and Electron Microscopy in the Porcine Retina" (Xie et al., 2018) [2]. This research data highlights our technique for retinal fundus image acquisition during spectral domain optical coherence tomography (SD-OCT) in a large animal model. Low and high magnification electron micrographs are included to demonstrate the ultrastructural features of the porcine retina. Data on horizontal tissue shrinkage during processing of the porcine retina are presented.

DOI of original article: https://doi.org/10.1016/j.exer.2018.08.003
* Corresponding author at: Department of Medical Physiology, Texas A&M University Health Science Center, Temple, TX, USA.
E-mail address: Robert.Rosa@BSWHealth.org (R.H. Rosa Jr.).

https://doi.org/10.1016/j.dib.2018.10.123

Specifications table

Subject area	*Biology*
More specific subject area	*Porcine retinal morphology*
Type of data	*Figures*
How data was acquired	*Imaging: Transmission electron microscopy of porcine retina using epoxy resin embedded tissue.* *in vivo imaging of retinal layers using Spectral Domain-Optical Coherence Tomography (Heidelberg Spectralis HRA + OCT).*
Data format	*Processed*
Experimental factors	*Domestic porcine retina without pretreatment.*
Experimental features	*The lamellar architecture of the porcine retina was examined with transmission electron microscopy and SD-OCT.*
Data source location	*Temple, Texas USA*
Data accessibility	*With this data paper.*
Related research article	*W. Xie, M. Zhao, S. Tsai, W.L. Burkes, L.B. Potts, W. Xu, H.R. Payne, T.W. Hein, L. Kuo, R.H. Rosa, Jr. Correlation of spectral domain optical coherence tomography with histology and electron microscopy in the porcine retina. Exp Eye Res. 177 (2018) 181–190.*

Value of the data

- The dataset demonstrates a technique for retinal fundus image acquisition during spectral domain optical coherence tomography (SD-OCT) in a large animal model.
- The data can be used to correlate the lamellar structure of the porcine retina using histology, transmission electron microscopy, and SD-OCT.
- The research community can employ these new data on SD-OCT interpretation to evaluate *in vivo* "histologic" changes in pig models of various retinal diseases.

1. Data

These data provide information regarding animal subject alignment for OCT image acquisition (Fig. 1) and a detailed morphologic analysis of the porcine retina using transmission electron microscopy (TEM) (Figs. 2–6) and correlation with images obtained *in vivo* using spectral domain optical coherence tomography (SD-OCT). SD-OCT image correlation with light microscopy and tissue shrinkage with histologic processing is also presented in these data sets (Fig. 7).

2. Materials and methods

For additional details on experimental design, please see the related research article [2].

2.1. Animals

A total of 9 domestic pigs (Sus scrofa domesticus, Yorkshire; male and female; age range, 8–12 weeks; weight, 10–20 kg) were examined.

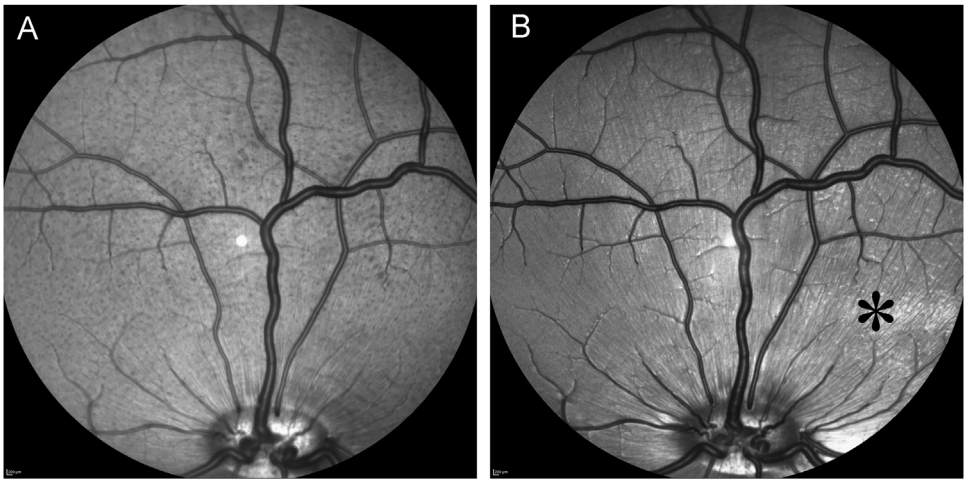

Fig. 1. Infrared and blue reflectance imaging of the porcine retina with alignment for OCT image acquisition. Porcine fundus images were acquired with infrared reflectance imaging (A) and blue reflectance imaging (B). Note the speckled pattern of choroidal pigment in the infrared image (A) and the high definition details of the retinal vasculature and the retinal nerve fiber layer (asterisk) in the blue reflectance image (B). Eye positioning during SD-OCT image acquisition can induce errors. The animal should be positioned with the superior retina located superiorly and the optic nerve head located inferiorly in the infrared image for OCT imaging as shown in A.

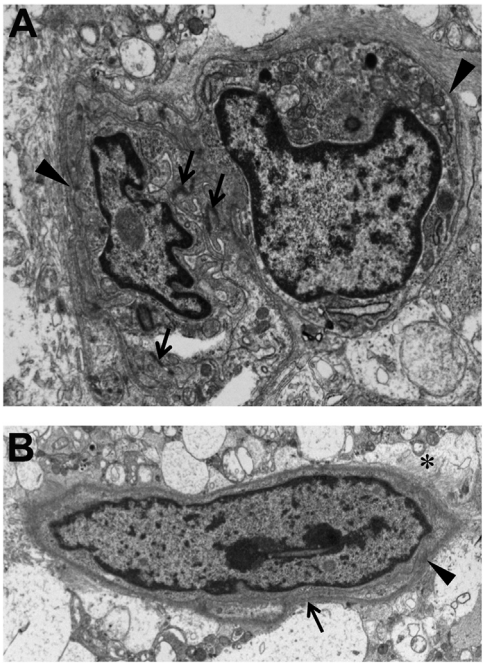

Fig. 2. TEM of endothelial cells and fibrous astrocyte in the inner plexiform layer. High magnification TEM (A) of upper left boxed area in Xie et al., 2018 (Figure 4A) showing endothelial cells with junctional densities (arrows) and basement membrane (arrowheads). High magnification TEM (B) of upper right boxed area in Xie et al., 2018 (Figure 4A) shows a fibrous astrocyte with patchy basement membrane (arrow), subplasmalemmal aggregates of microfilaments (arrowhead), and fine collagenous fibrils (asterisk) arranged perpendicular to the basement and plasma membranes. These cell types, in addition to amacrine and Müller cells, corresponded to a discontinuous relative hypo-reflective band in the inner plexiform layer. Scale bar: 1 micron.

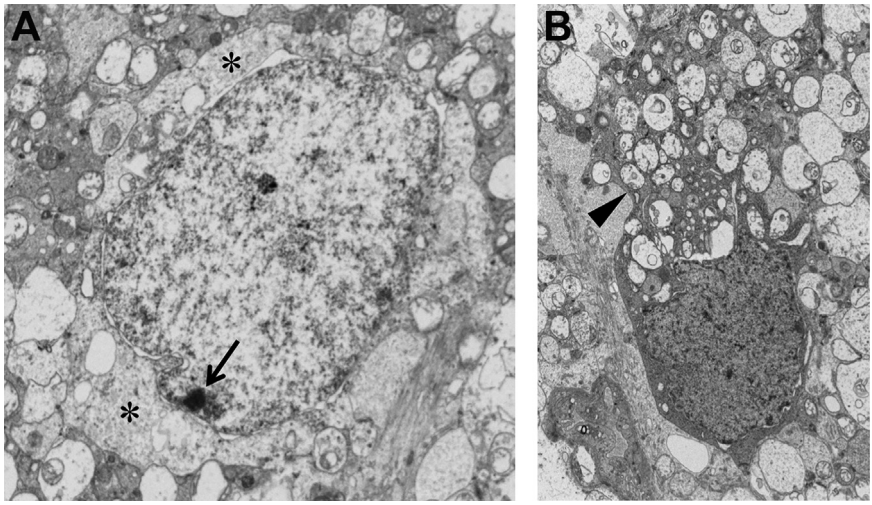

Fig. 3. TEM of amacrine and müller cells in the inner plexiform layer. High magnification TEM of an amacrine cell (A) and a Müller cell (B) located in the middle aspect of the inner plexiform layer. Note the lucent cytoplasm (asterisks), dispersed nucleoplasm, and small nucleolus (arrow) in the amacrine cell (A) and the extensive network of relatively electron dense cytoplasmic processes (arrowhead) of the Müller cell wrapping around other cytoplasmic processes in the inner plexiform layer. These cell types, in addition to endothelial cells and fibrous astrocytes, appeared to correspond to a discontinuous relative hypo-reflective band in the inner plexiform layer. Scale bars: A, 2 microns; B, 5 microns.

2.2. Tissue preparation for morphological analyses

After enucleation, eyes were immediately placed in 4% paraformaldehyde (PFA), followed by dissection and post-fixation of the posterior segment in 2% PFA/2% glutaraldehyde in phosphate-buffered saline (PBS) at 4 °C for 48 h.

2.3. Epoxy resin embedding and sectioning

A 3 mm-wide strip of retina-choroid-sclera was dissected along the vertical meridian, including optic nerve head and ora serrata. Following secondary fixation in buffered 1% osmium tetroxide and tissue processing, the retina-choroid-sclera tissue segment was embedded in Eponate 12 resin (Ted Pella, Redding, CA). Tissue blocks were then cut into 500 nm-thick sections using the RMC Power-Tome X Ultramicrotome (Boeckeler Instruments, Tucson, AZ). After staining with 1% toluidine blue (Sigma-Aldrich, St. Louis, MO) and coverslipping, the tissue was examined with light microscopy.

2.4. Transmission electron microscopy

Tissue preparation and processing for transmission electron microscopy (TEM) was performed as previously described [1]. Ultrathin (80 nm-thick) sections of the retina-choroid-sclera were examined with an FEI Morgagni 268 transmission electron microscope. A MegaViewIII camera with iTEM software (Olympus Soft Imaging Systems, Germany) was employed to record TEM images at magnifications of 1800 × to 44,000 ×.

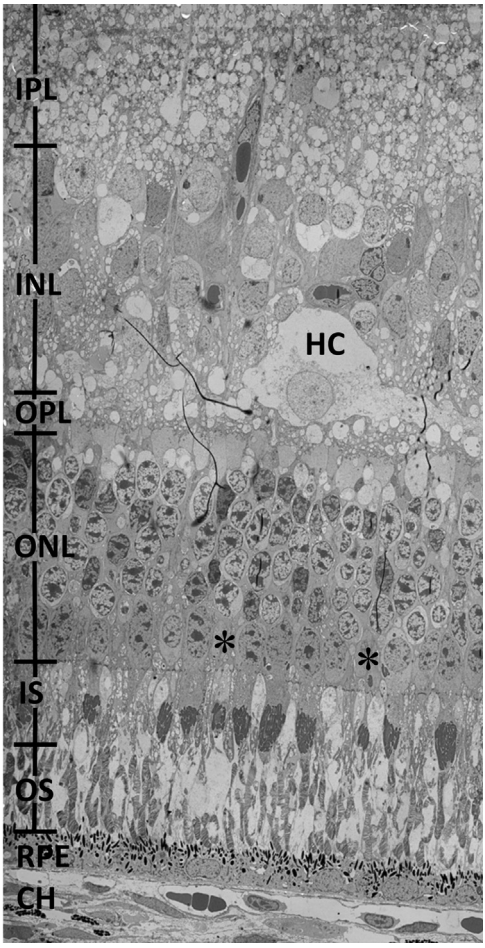

Fig. 4. Low magnification TEM of the porcine retina. Note the large horizontal cell (HC) in the outer aspect of the inner nuclear layer (INL), the Müller cell body (MC) in the inner aspect of the INL, and the deep retinal capillaries (arrowheads). Cone nuclei (asterisk) were concentrated in the outer aspect of the outer nuclear layer (ONL) and corresponded to a relative hypo [HYPHEN]reflective band in the ONL. Other abbreviations: IPL, inner plexiform layer; OPL, outer plexiform layer; IS, inner segments; OS, outer segments; CH, choroid. Scale bar: 10 microns.

2.5. SD-OCT image acquisition

The Heidelberg Spectralis HRA+OCT with the software Heidelberg Eye Explorer (HEYEX version 6.6, Heidelberg, Germany) was employed to image the retina along the vertical meridian through the optic nerve head as described in Xie et al. [2]. Signal quality was at least 25 db, and 100 frames were averaged per B-scan. Scans were acquired at a speed of 40,000 A-scans per second, and each two-dimensional B-scan contained up to 1536 A-scans.

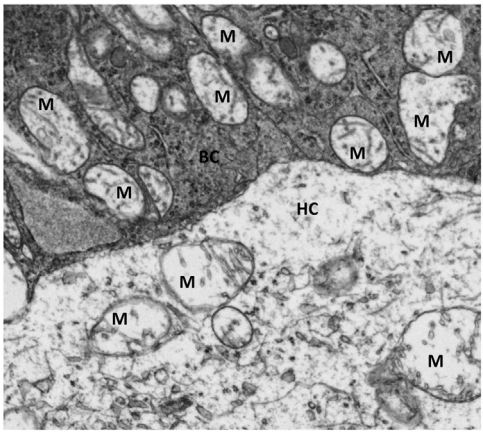

Fig. 5. TEM of bipolar cell and horizontal cell cytoplasm. High magnification TEM of boxed area in Xie et al. [2] (Fig. 4C) shows numerous mitochondria (M) in bipolar (BC) and horizontal (HC) cells in the inner nuclear layer. The mitochondria in these cells appeared to correspond to a hyper-reflective band in the middle of the inner nuclear layer on SD-OCT. Scale bar: 1 micron.

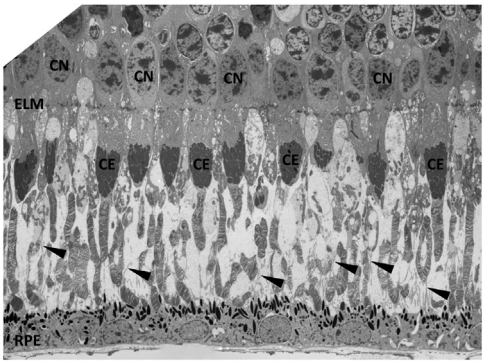

Fig. 6. TEM of outer retina and retinal pigment epithelium. The RPE cells exhibited long apical cytoplasmic cell processes (arrowheads) which were intimately associated with the photoreceptor outer segments in the interdigitation zone. Some of the RPE apical cell processes appeared to extend to near the photoreceptor inner-outer segment junction. Abbreviations: cone nuclei, CN; external limiting membrane, ELM; cone ellipsoid, CE; retinal pigment epithelium, RPE. Scale bar: 10 microns.

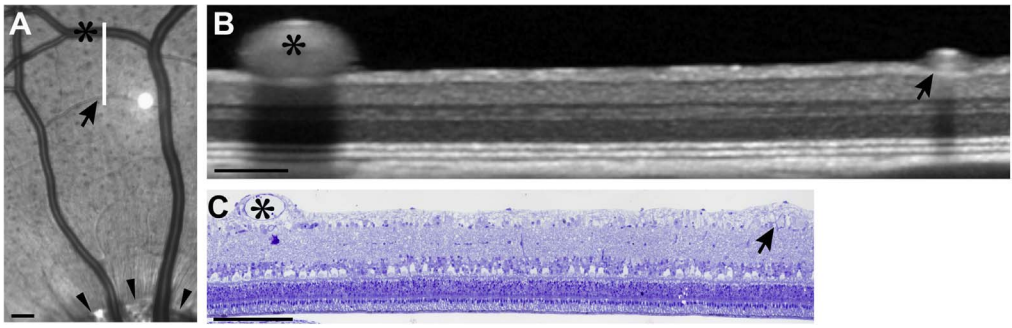

Fig. 7. SD-OCT-histology correlation and horizontal tissue shrinkage. Infrared reflectance imaging of porcine retina (A) demonstrates the scanned area (white line) in the superior retina, including a branch retinal vein (asterisk) and a branch retinal arteriole (arrow). Note the superior margin of the optic nerve head (arrowheads). The SD-OCT image (B) shows the same larger (asterisk) and smaller (arrow) retinal vessels displacing the internal limiting membrane (ILM) toward the vitreous. A toluidine blue-stained epoxy resin embedded section (C) obtained from the corresponding retina reveals that the larger vessel (asterisk) is a large branch retinal venule and the smaller vessel (arrow) is a small branch retinal arteriole. Note the corresponding inward displacement of the ILM toward the vitreous by the retinal vessels in the SD-OCT and histologic images (B, C). There is apparent lateral or horizontal (but not vertical) tissue shrinkage (B, C) after histologic processing. Incongruity in the measurements of the horizontal length of the retina in the OCT image vs. the photomicrograph might be due, in part, to image stretching or distortion associated with SD-OCT algorithmic image processing. Scale bars: A, 500 microns; B and C, 200 microns.

Acknowledgements

Supported by the Liles Macular Degeneration Research Fund, Kruse Chair Endowment, Baylor Scott & White-Central Texas Foundation, Ophthalmic Vascular Research Program of Baylor Scott & White Health, Retina Research Foundation and NIH NEI R01EY024624 and R21EY024406.

Transparency document. Supporting information

Transparency data associated with this article can be found in the online version at https://doi.org/10.1016/j.dib.2018.10.123.

References

[1] P.A. Scott, H.J. Kaplan, J.H. Sandell, Anatomical evidence of photoreceptor degeneration induced by iodoacetic acid in the porcine eye, Exp. Eye Res. 93 (2011) 513–527. https://doi.org/10.1016/j.exer.2011.06.017 https://doi-org.ezproxy.library.tamu.edu.

[2] W. Xie, M. Zhao, S. Tsai, W.L. Burkes, L.B. Potts, W. Xu, H.R. Payne, T.W. Hein, L. Kuo, R.H. Rosa Jr., Correlation of spectral domain optical coherence tomography with histology and electron microscopy in the porcine retina, Exp. Eye Res. 177 (2018) 181–190. https://doi.org/10.1016/j.exer.2018.08.003.